

Resting-state global functional connectivity as a biomarker of cognitive reserve in mild cognitive impairment

N. Franzmeier¹  · M. Á. Araque Caballero¹ · A. N. W. Taylor¹ · L. Simon-Verrot¹ · K. Buerger^{1,2} · B. Ertl-Wagner³ · C. Mueller¹ · C. Catak¹ · D. Janowitz¹ · E. Baykara¹ · B. Gesierich¹ · M. Duering¹ · M. Ewers¹ · for the Alzheimer's Disease Neuroimaging Initiative

Published online: 5 October 2016

© Springer Science+Business Media New York 2016

Abstract Cognitive reserve (CR) shows protective effects in Alzheimer's disease (AD) and reduces the risk of dementia. Despite the clinical significance of CR, a clinically useful diagnostic biomarker of brain changes underlying CR in AD is not available yet. Our aim was to develop a fully-automated approach applied to fMRI to produce a biomarker associated with CR in subjects at increased risk of AD. We computed resting-state global functional connectivity (GFC), i.e. the average connectivity strength, for each voxel within the cognitive control network, which may sustain CR due to its central role in higher cognitive function. In a training sample including 43 mild cognitive impairment (MCI) subjects and 24

healthy controls (HC), we found that MCI subjects with high CR (> median of years of education, CR+) showed increased frequency of high GFC values compared to MCI-CR- and HC. A summary index capturing such a surplus frequency of high GFC was computed (called GFC reserve (GFC-R) index). GFC-R discriminated MCI-CR+ vs. MCI-CR-, with the area under the ROC = 0.84. Cross-validation in an independently recruited test sample of 23 MCI subjects showed that higher levels of the GFC-R index predicted higher years of education and an alternative questionnaire-based proxy of CR, controlled for memory performance, gray matter of the cognitive control network, white matter hyperintensities, age, and gender. In conclusion, the GFC-R index that captures GFC changes within the cognitive control network provides a biomarker candidate of functional brain changes of CR in patients at increased risk of AD.

Keywords Cognitive reserve · Biomarker · Mild cognitive impairment · Alzheimer's disease · Global functional connectivity · Resting-state fMRI

Data used in preparation of this article were obtained from the Alzheimer's Disease Neuroimaging Initiative (ADNI) database (adni.loni.usc.edu). As such, the investigators within the ADNI contributed to the design and implementation of ADNI and/or provided data but did not participate in analysis or writing of this report. A complete listing of ADNI investigators can be found at: http://adni.loni.usc.edu/wp-content/uploads/how_to_apply/ADNI_Acknowledgement_List.pdf

Electronic supplementary material The online version of this article (doi:10.1007/s11682-016-9599-1) contains supplementary material, which is available to authorized users.

✉ N. Franzmeier
nicolai.franzmeier@med.uni-muenchen.de

¹ Institut für Schlaganfall-und Demenzforschung (ISD), Ludwig-Maximilians-Universität LMU, Klinikum der Universität München, Feodor-Lynen Straße 17, 81377 Munich, Germany

² German Center for Neurodegenerative Diseases (DZNE, Munich), Feodor-Lynen Straße 17, 81377 Munich, Germany

³ Institute for Clinical Radiology, Klinikum der Universität München, Ludwig-Maximilian University, Marchioninistraße 15, 81377 Munich, Germany

Introduction

Cognitive reserve (CR) refers to the ability to cognitively perform relatively well in the presence of brain pathology (Stern 2002, 2009). Life-time experiences - such as education and occupational attainment - or IQ are commonly used as proxy measures of CR (Stern 2009). In Alzheimer's disease (AD), higher levels of such CR proxies are associated with higher cognitive performance relative to the level of brain damage, such as measured by cerebral FDG-PET hypometabolism or impaired blood flow (Bastin et al. 2012; Boots et al. 2015; Ewers et al. 2014; Scarmeas et al. 2003; Stern et al. 1992, 1995), grey matter atrophy (Bastin et al. 2012; Boots et al.

2015), white matter damage (Brickman et al. 2011), and primary pathologies including amyloid-beta ($A\beta$) and tau (Rentz et al. 2010; Vemuri et al. 2011, 2015). These results suggest that higher levels of CR as measured by education and other proxies are associated with a higher ability to cope with brain pathology in AD.

Compensatory functional brain changes that may underlie CR have been investigated in a number of task-related fMRI studies (Stern et al. 2005, 2008) or resting-state fMRI studies in HC subjects (Arenaza-Urquijo et al. 2013). Task-related fMRI studies in MCI and AD revealed an association between increased CR proxies (education, occupation) and higher brain activation (Bosch et al. 2010; Solé-Padullés et al. 2009). However, task-fMRI is often difficult to perform for cognitively impaired patients, and may thus not be suitable for clinical use to assess CR in AD. From a clinical point of view, a major question is whether simple measures of basic brain function are indicative of CR, and thus could be used as a marker of CR-related brain changes in AD. The need of a biomarker of CR-related brain changes is urgent in view of a growing number of clinical trials that target protective brain mechanisms in AD, such as cognitive training or meditation (Buschert et al. 2011; Reijnders et al. 2013; Schultz et al. 2015; Wells et al. 2013).

The overall goal of the current study was to develop a neuroimaging-based diagnostic biomarker of functional brain changes underlying CR in subjects with mild cognitive impairment (MCI). We specifically chose a sample of MCI subjects since CR-related functional brain changes may most likely become apparent at a stage of emerging brain pathology, such as in MCI (Stern 2002). We focused on resting-state global functional connectivity (GFC, also known as weighted degree centrality) within the cognitive control network as a measure of functional brain processes of CR. The rationale for selecting the cognitive control network to subservise CR is based on its' link to CR proxies (Cole et al. 2012), its' task-invariant role in cognition (Cole et al. 2013), and its' suggested compensatory function in early AD (Elman et al. 2014; Oh et al. 2015). The cognitive control network includes major brain hubs with high GFC (Cole et al. 2010), where greater GFC has been previously associated with higher IQ, i.e. a proxy of CR, in young subjects. In the current study, CR was measured by the proxy of years of education, which is the best validated CR proxy measure to date in AD (Stern 2012).

Using a cross-validation approach, we compared the frequency distribution of GFC values within the cognitive control network between MCI subjects with high CR (more years of education) to MCI with low CR (lower years of education) and HC groups. A newly developed summary index that detects GFC frequency differences between MCI subjects with low and MCI subjects with high CR, henceforth called GFC reserve (GFC-R) index, was tested as a marker of CR in an independent validation sample of MCI subjects. We hypothesized firstly that MCI subjects with more years of education

show an increased number of relatively high GFC values within the cognitive control network compared to MCI subjects with less years of education. Secondly, we hypothesized that higher levels of the GFC-R index are predictive of more years of education and a second questionnaire based CR proxy in the validation sample of MCI subjects. Thirdly, we hypothesized that the GFC-R index is specifically related to CR proxies and not driven by pathological brain changes such as amyloid-beta deposition, cerebral small vessel disease or grey matter atrophy.

Methods

Subjects

We included two independent samples each of amnesic MCI and HC subjects to cross-validate our findings. The training sample included 24 amyloid-PET negative ($A\beta^-$) HC subjects and 43 Amyloid-PET positive ($A\beta^+$) patients with amnesic MCI. Amyloid PET status was defined based on pre-established cut-off values of global [^{18}F] AV-45 PET standardized uptake value ratio (for $A\beta^-$ = global AV-45 PET SUVR < 1.11) (Landau et al. 2013). All data were downloaded from the Alzheimer's Disease Neuroimaging Initiative (ADNI) database, freely accessible for researchers (<http://adni.loni.usc.edu/>). ADNI was launched in 2003 as a public-private partnership, led by Principal Investigator Michael W. Weiner, MD. The primary goal of ADNI has been to test whether serial MRI, PET, other biological markers, and clinical and neuropsychological assessment can be combined to measure and predict the progression of MCI and early AD (www.adni-info.org).

The test sample comprised 32 HC subjects as well as 23 subjects with amnesic MCI, recruited between 2014 and 2015 at the memory clinic of the Institute for Stroke and Dementia Research (ISD) at the Klinikum der Universitaet Muenchen in Germany.

For the ISD study, the inclusion criteria were defined as follows: 1) age >60 years, 2) no signs of depression, 3) no presence or history of neurological or psychiatric disorders (except for MCI), 4) no presence or history of alcohol or drug abuse, 5) no diabetes mellitus, 6) no MRI contraindications. All subjects underwent structural MRI, resting-state fMRI and cognitive testing using the CERAD-Plus test battery (Luck et al. 2009). A subject was defined as HC, when reporting no subjective memory complaints and scoring within 1.5 standard deviations (SD) of the age, gender and education adjusted norms in all subtests of the CERAD-Plus battery (Luck et al. 2009). MCI was diagnosed according to the Petersen criteria (Petersen 2004), when scoring 1.5 SD below the age, gender and education adjusted norms in at least one of the learning or recall subtests of the CERAD-Plus battery.

For the training sample (ADNI), details about the inclusion can be found online (<https://adni.loni.usc.edu/wp-content/uploads/2008/07/adni2-procedures-manual.pdf>). Similar to the diagnosis of MCI in the ISD sample, MCI was diagnosed in ADNI according to the Petersen criteria (Petersen 2004).

Cognitive reserve and neuropsychological assessment

The number of years of formal education was used as a proxy for CR in both samples. In the test sample (ISD) we additionally used the cognitive reserve index questionnaire (Nucci et al. 2012) as a second proxy of CR. The CRIq is a standardized questionnaire based measure for the assessment of CR that combines information about education, working activity and leisure time. For neuropsychological assessments, memory performance was assessed using memory tests that were comparable between the ADNI and the ISD sample. As a measure of episodic memory performance, the total score of the CERAD word list learning tests was assessed in the ISD sample (Luck et al. 2009), and the total score of the Rey Auditory Verbal Learning Test (RAVLT) in the ADNI sample (Schoenberg et al. 2006). Both tests are designed as list-learning paradigms in which the patient is read a list of words by the examiner in several trials (CERAD: 10 words in 3 trials; RAVLT: 15 words in 5 trials) and is asked to recall as many words from the list as possible after each trial. The total score reflects the number of words correctly remembered cumulated across trials.

MRI acquisition

Training sample (ADNI)

All MRI scans were performed on Philips 3 T MRI scanners, using an 8-channel head matrix coil. High-resolution T1-weighted scans were acquired using a 3D MP-RAGE sequence, with whole brain coverage and a voxel resolution of $1 \times 1 \times 1.2$ mm. Fluid attenuated inverse recovery (FLAIR) scans were obtained with a voxel resolution of $0.86 \times 0.86 \times 5$ mm. Resting-state-fMRI images were acquired using a single shot T2*-weighted EPI sequence collecting 140 volumes, with a TR of 3000 ms, a flip angle of 80° and 3.3 mm isotropic voxel resolution. Prior to the resting-state scan, subjects were instructed to keep their eyes open.

Test sample (ISD)

All MRI scans were performed on a Siemens Verio 3 T MRI scanner using a 32-channel head coil. For each subject a structural image was obtained using a high-resolution 3D MPRAGE T1-weighted sequence with 1 mm isotropic voxel resolution. Using the same field of view and voxel dimensions FLAIR images were recorded. Functional resting-state images

were acquired using a T2*-weighted echo-planar imaging (EPI) pulse sequence collecting 180 volumes with a TR = 2580 ms, flip angle = 80° and 3.5 mm isotropic voxel resolution. Prior to the resting-state scan the subjects were instructed to keep their eyes closed and not to fall asleep during the scanning procedure. Using the same field of view as the functional resting-state images, field maps were acquired (TE = 7.38/4.92 ms, TR = 675 ms) to correct for susceptibility artifacts and inhomogeneity of the magnetic field during preprocessing of the resting-state data.

Spatial normalization of MRI scans

The spatial normalization of the MRI scans was done separately for both samples, following the same protocol of image processing based on SPM 12 (Wellcome Trust Centre for Neuroimaging, University College London, United Kingdom: www.fil.ion.ucl.ac.uk/spm). T1-weighted images were segmented into probabilistic maps of grey matter, white matter and cerebrospinal fluid maps through the SPM's new-segment approach (Ashburner and Friston 2005). Next, the spatial normalization parameters were estimated using a high-dimensional diffeomorphic registration algorithm to warp each subjects' grey matter map to a group-specific grey matter template that was defined in an iterative procedure, as implemented in SPM's DARTEL toolbox (Ashburner 2007). Subsequently, the group-specific template was registered to the MNI template in order to estimate the affine transformation parameters. Next, the non-linear (DARTEL flow-fields) and the affine transformation parameters were combined and applied to the segmented grey matter maps, so that all grey matter images were spatially normalized to the MNI space. The spatially-normalized grey matter maps were averaged and binarized at a voxel value >0.3 to create a group-specific grey matter mask for later fMRI functional connectivity analyses. Similarly, we averaged and binarized the spatially-normalized white-matter (binarized at threshold >0.9) and cerebrospinal-fluid (binarized at threshold >0.7) that were used during preprocessing of the resting-state fMRI data. For later extraction of grey matter volume, we created spatially normalized grey matter maps for each subject, that were smoothed with a 8-mm full-width at half-maximum (FWHM) Gaussian kernel and modulated to preserve the volume of the images.

WMH volume assessment

The assessment of WMH volume was conducted separately for both samples but following the same protocol. In a first step, FLAIR images were registered to the T1-weighted images and segmented into three tissue-probability maps. Subsequently, a histogram-segmentation (Otsu 1979) was conducted to separate WMH from confounding cerebrospinal

fluid voxels. The resulting WMH segmentations were manually edited by two independent raters in order to remove voxels that were misclassified as WMH. The inter-rater reliability of the WMH assessment yielded a Dice coefficient of 0.98. For each subject, WMH volume was computed as the volume of WMH divided by the total brain volume.

Preprocessing of resting-state fMRI

The preprocessing of both samples was done separately, but following the same protocol. The first 10 volumes of each subjects' resting-state scan were discarded to allow for equilibration of the magnetic field. All remaining volumes were realigned to the first volume to correct for motion, coregistered to native-space T1-weighted images and smoothed using an 8 mm FWHM Gaussian kernel. None of the subjects' motion parameters exceeded 2 mm translations or 2° rotations. For the ISD-sample, there was additional slice-timing and field map correction. Next, the DARTEL flow-fields and affine registration parameters that were estimated during preprocessing of the T1-weighted images were combined and applied to all resting-state fMRI volumes to spatially normalize the images to MNI space. The spatially normalized fMRI images were further detrended and band-pass filtered, using a frequency band of 0.01–0.08 Hz. In a second step we regressed out the 6 motion parameters (3 translations, 3 rotations) and the BOLD signal averaged across the white matter and cerebrospinal fluid masks that were created during preprocessing of the T1-weighted images.

Assessment of GFC

For each subject, GFC was determined based on the preprocessed and spatially normalized resting-state fMRI scans, following a previously established protocol (Cole et al. 2012). For each voxel in the grey matter, the GFC was determined by computing seed-based Pearson-Moment correlations of the BOLD signal changes between the seed voxel and each of the other voxels within the grey matter (as defined by the customized grey matter mask). For each seed voxel, only Pearson-Moment correlation coefficients with $r > 0$ were retained, Fisher z-transformed and averaged across the voxels within the grey-matter-mask space to obtain the GFC coefficient. This resulted in a 3D brain map of GFC coefficients for each subject. Note that we included only positive correlation coefficients for computing the GFC, because positive and negative correlations may cancel each other out when averaging the correlation coefficients. More precisely, if a voxel shows high positive connectivity to brain area A and high negative connectivity to brain area B, averaging both values would result in a small if not zero correlation coefficient, which would be falsely interpreted as low connectivity.

Thus, in line with a previous study (Cole et al. 2012), we focused on positive connectivity values only.

Spatial maps of resting-state networks

The cognitive control network covers the anterior cingulate cortex, dorsolateral prefrontal cortex, anterior insular cortex, dorsal premotor cortex and posterior parietal cortex (Cole et al. 2013, 2014a; Cole and Schneider 2007). For the current study, we determined the spatial boundaries of the cognitive control network based on an a-priori conducted meta-analysis in order to avoid a sample specific bias in the spatial definition of the network. The meta-analysis was conducted using NeuroSynth, a web-based tool for fully automated detection of brain activation coordinates from published task-fMRI data (<http://www.neurosynth.org>). By entering a search term in the NeuroSynth database, brain activation associated with the search term entered is analyzed across studies, yielding a probabilistic map of brain activation related to that term (Yarkoni et al. 2011). For the current study, we used “cognitive control” as a search term, yielding a z-scored probability map based on 428 task-fMRI studies (as of September 14, 2015). In order to obtain a reliable map of the cognitive control network we applied a false discovery rate corrected p-threshold of $p(\text{FDR}) < 0.01$ (see Fig. 1). The spatial map of the cognitive control network was additionally masked with the group-specific grey matter masks for each sample separately in order to restrict all further analyses to voxels that had a high likelihood of falling within the grey matter. We performed control analyses on 7 major brain networks (Yeo et al. 2011), to test whether a relationship between CR and GFC was specific to the cognitive control network. Accordingly, we downloaded the 7 network parcellations that are freely available online

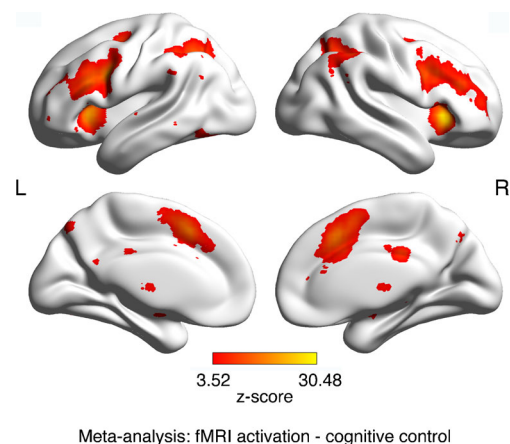


Fig. 1 Meta-analytical activation map across 428 task-fMRI studies that were associated with search term “cognitive control” (FDR-corrected at $p < 0.01$) in NeuroSynth, projected on a brain surface. Colors indicate z-scores

(ftp://surfer.nmr.mgh.harvard.edu/pub/data/Yeo_JNeurophysiol11_MNI152.zip). Again, all 7 networks were additionally masked with the group specific grey matter masks for each sample. To control for potentially confounding effects of brain atrophy, we extracted the grey matter volume within the network masks for each subject, applied to the modulated smoothed and normalized grey matter images that were created during the preprocessing of structural MRI images.

Generation of GFC index related to CR (GFC-R index)

Study design

Our aim was to develop a summary index to quantify GFC frequency changes within the cognitive control network that were associated with the CR proxy years of education in patients with MCI. In brief, the ADNI sample served as a training sample to create the GFC-R index that is related to our CR proxy *education*. Subsequently, we tested the validity of this GFC based index as a predictor of the CR proxy years of education and the CR-questionnaire (CRIq) composite score in the ISD sample, which served as an independent test sample. A Flow diagram illustrating the individual steps to create the GFC-reserve index is shown in Fig. 2.

Dichotomization of subjects according to CR

The HC and MCI groups were each dichotomized into groups of low and high CR (CR- vs CR+), split at the median of years of education within the entire sample. The groups were dichotomized separately within the ISD (CR+: > median education = 13) and the ADNI sample (CR+: > median education = 16).

Histogram analysis of GFC

For each diagnostic group (MCI vs. HC) within the CR+ and CR- subjects, we plotted a histogram of the GFC frequencies across voxels of the cognitive control network (Fig. 2a and b). Visual inspection of the histograms in the training sample (ADNI) revealed, that the GFC histogram of the MCI CR- subjects showed an overall shift to the left of the HC subjects, with a decreased frequency of relatively high GFC values, but an increase of lower GFC values compared to the HC CR- group (Fig. 2b). Conversely, the GFC histogram of the MCI CR+ subjects showed a shift to the right of the HC CR+ group.

In a next step, we binned the GFC voxel values for each subject at intervals of 0.01 from $z = 0$ to $z = 0.6$ resulting in a total of 60 bins, each containing the number of voxels (i.e. the GFC frequency) falling within that bin. To quantify changes in GFC frequency in MCI with respect to the HC group, we bin-wise subtracted each MCI CR+ subject's GFC frequencies

from the averaged GFC frequencies in the HC CR+ group. The analogous subtraction was done for the MCI CR-, where each MCI subject's histogram was subtracted from the average histogram of the HC CR- group. Thus, for each MCI CR group, alterations of GFC frequencies (called GFC-Diff, Fig. 2c) were obtained according to the following equation.

$$GFC-Diff_{ijk} = GFCfrequency(MCI)_{ijk} - Mean\ GFCfrequency(HC)_{ik} \quad (1)$$

where, $i =$ CR group (CR+ or CR-), $j =$ MCI subject, $k =$ GFC bin (1–60).

In bins where a MCI subject had a higher GFC frequency than the HC group, GFC-Diff values were positive (green shaded area in Fig. 2c–e). Conversely, in bins where a MCI subject showed a lower GFC frequency compared to the HC group, the GFC-Diff score was negative (red shaded area in Fig. 2c–e). To identify GFC bins where MCI CR+ and MCI CR- subjects showed different GFC frequency changes, we compared GFC-Diff scores between the CR groups for each of the 60 bins, using two-sample t-tests with the significance threshold being $\alpha = 0.05$ for each t-test (Fig. 2d). We did not correct for multiple testing at this stage, since the analysis was an intermediate step, exclusively done in order to select bins where MCI CR- and MCI CR+ groups differed in terms of GFC-Diff.

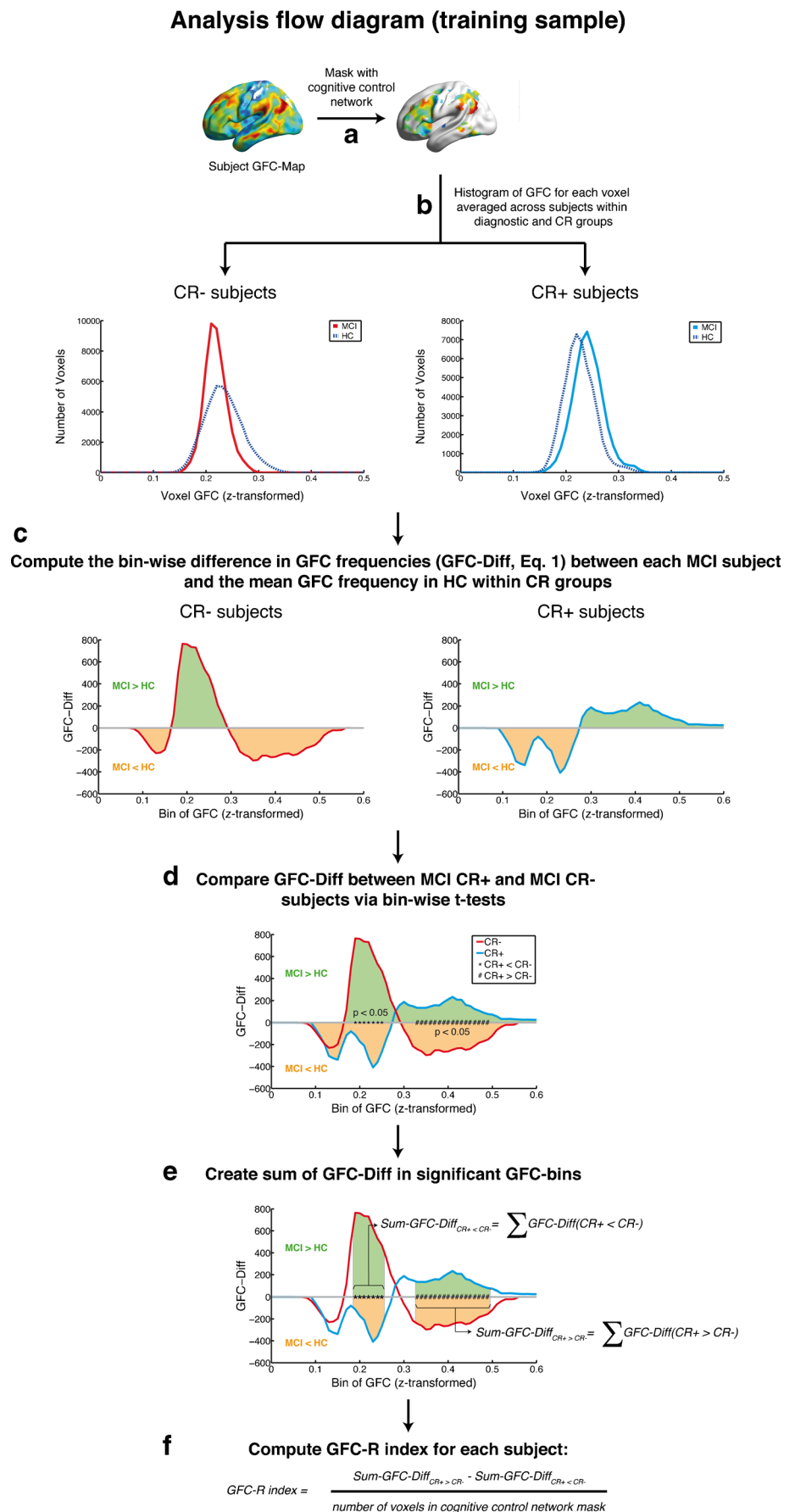
The results of the t-tests showed that GFC-Diff scores were greater (i.e. more positive) in MCI CR+ compared to MCI CR- in the range from 0.34 to 0.5, suggesting that MCI CR+ had significantly increased frequencies of relatively high GFC values (henceforth referred to as $GFC-Diff_{CR+>CR-}$) relative to MCI CR- subjects. In contrast, GFC-Diff scores were increased in MCI CR- compared to MCI CR+ subjects in a range from 0.2 to 0.26, suggesting that MCI CR- subjects had a higher frequency of relatively low GFC values (henceforth referred to as $GFC-Diff_{CR+<CR-}$) compared to MCI CR+ subjects. In order to create a subject-specific summary score of GFC frequency differences indicative of CR+ status, we subtracted the sum of GFC-Diff values in the $GFC-Diff_{CR+<CR-}$ from the sum of GFC-Diff values in the $GFC-Diff_{CR+>CR-}$. Finally, this differences was divided by the total number of voxels in the cognitive control network mask to standardize it to a range between -1 and 1 (Fig. 2e and f, Eq. 2).

$$GFC-Rindex_j = \frac{\sum GFC-Diff_{CR+>CR-} - \sum GFC-Diff_{CR+<CR-}}{\text{Number of voxels in mask}} \quad (2)$$

where $j =$ subject

This coefficient was then used as our GFC-R index. A negative GFC-R index indicates an increased GFC frequency in $GFC-Diff_{CR+<CR-}$ and a simultaneous decrease in $GFC-Diff_{CR+>CR-}$, i.e. a MCI CR- characteristic pattern. Conversely a positive GFC-reserve indicates an increased GFC frequency in $GFC-Diff_{CR+>CR-}$ and a decreased frequency in $GFC-Diff_{CR+<CR-}$, a pattern that was typically seen in MCI CR+.

Fig. 2 Analysis flow diagram, illustrating the steps of GFC-R index computation. **a** Voxel-wise GFC is computed based on preprocessed resting-state fMRI for each subject and masked with the binarized cognitive control network map. **b** The GFC frequency distribution within the cognitive control network is plotted for groups split by diagnosis (HC & MCI) and CR status (CR- & CR+). **c** GFC within the cognitive control network is binned in intervals of 0.01 for each subject. Within each CR group, the difference in GFC differences (GFC-Diff) between each MCI subject and the average GFC within the HCs group is computed. Colored areas indicate whether MCI subjects showed lower (*red*) or higher (*green*) GFC frequency than the HC subjects. **d** GFC-Diff scores are compared between MCI CR+ and MCI CR- groups via bin-wise two-sample t-tests. **e** GFC-Diff scores are summed up across the selected bins for each MCI subject. In order to create a subject-specific summary score of GFC frequency differences indicative of CR+ status, the sum of GFC-Diff values in the GFC-Diff_{CR+<CR-} was subtracted from the sum of GFC-Diff values in the GFC-Diff_{CR+>CR-}. **f** This differences was divided by the total number of voxels in the cognitive control network mask to standardize it to a range between -1 and 1 to derive the GFC-R index for each MCI subject



All steps described above were conducted also for the test sample (ISD). Supplementary Figure 1 is showing – equivalent to Fig. 2b – the distribution of GFC voxels averaged across subjects within CR and diagnostic (MCI vs. HC) groups. When conducting the t-tests to compare the GFC-Diff values between MCI CR+ and MCI CR-, we found $\text{GFC-Diff}_{\text{CR+}<\text{CR-}}$ in a range from 0.2 to 0.22 (vs. 0.2–0.26 in the training sample) and the $\text{GFC-Diff}_{\text{CR+}>\text{CR-}}$ in a range from 0.29 to 0.41 (vs. 0.34–0.5 in the training sample). The $\text{GFC-Diff}_{\text{CR+}<\text{CR-}}$ fully overlapped between both samples, whereas the $\text{GFC-Diff}_{\text{CR+}>\text{CR-}}$ only partly overlapped. For our validation analysis, we used the $\text{GFC-Diff}_{\text{CR+}>\text{CR-}}$ and $\text{GFC-Diff}_{\text{CR+}<\text{CR-}}$ ranges derived from the training sample to compute the GFC-R index in the test sample. All above delineated steps were conducted accordingly for 7 major brain networks derived from a previous publication to control whether a relationship between CR and GFC was specific for the cognitive control network. Again, $\text{GFC-Diff}_{\text{CR+}>\text{CR-}}$ and $\text{GFC-Diff}_{\text{CR+}<\text{CR-}}$ ranges were assessed in the training sample and used to create the GFC-R index in the test sample. The histogram analysis was conducted fully-automated using in-house MATLAB scripts.

Statistical analysis

Demographic variables were compared between groups using t-tests for continuous variables and χ^2 -test for gender.

In order to test whether the GFC-R index differed between MCI CR+ vs. MCI CR- groups in the training sample, we conducted an ANCOVA, with group as the predictor, and age, gender, the global AV45 uptake, the grey matter volume within the cognitive control network, WMH volume and the learning score of the RAVLT as covariates. To evaluate how accurately the GFC-R index classified between MCI CR+ and MCI CR- subjects we performed a Receiver Operating Characteristic (ROC) Curve analysis. Prediction accuracy was quantified using the area under the curve (AUC). The 95 % Confidence interval (CI) for each ROC was computed with 2000 stratified bootstrap replicates for each ROC analysis. Equivalent models were run in the test sample, with the exception of AV45 PET uptake, which was not available in the ISD test sample.

Lastly, we tested whether the GFC-R index predicted the CR proxies (years of education, CRiQ) in the MCI subjects of the test sample (pooled across CR+ and CR-). To this end we conducted a multiple regression analysis, with the GFC-R index as a predictor of years of education or the CRiQ, controlled for age, gender, WMH volume, the learning score of the CERAD and the total grey matter volume within the cognitive control network. For the ADNI sample, the association between the continuous AV-45 PET measure, WMH volume and GFC-R was tested in the MCI subjects (who were by definition of the inclusion criteria all AV-45 PET positive).

We conducted a linear regression analysis, with WMH volume and AV45 uptake as independent variable and the GFC-R index as dependent variable, and age, gender, the RAVLT learning score and grey matter volume as nuisance covariates. An equivalent model was run for the ISD sample with the exception that AV45 was not available and that the CERAD word list learning score was entered as a covariate. To test whether the GFC-R index was related to cognitive performance, we applied linear regression, with the RAVLT learning score (ADNI) or the CERAD word list learning score (ISD) as a dependent variable and the GFC-R index as an independent variable, controlling for age, gender, as well as WMH volume and grey matter volume of the cognitive control network. Next, we tested whether our findings on the GFC-R for the prediction of years of education were specific for the cognitive control network. Thus, the regression analyses on GFC-R were repeated for each GFC-R index derived on the GFC frequencies in one of 7 major functional brain networks (i.e. Default Mode Network (DMN), Visual Network, Somatomotor Network, Dorsal Attention Network (DAN), Ventral Attention Network (VAN), Limbic Network, Frontoparietal Network (FPAN)) (Yeo et al. 2011).

All statistical analyses were conducted using the statistical software package *R* (R Development Core Team 2013). Linear models were computed using the `lm` command in *R*. Linear model assumptions (skewness, kurtosis, heteroscedasticity) were tested using the `gvlma` function implemented in *R*. For all models reported, no significant ($\alpha = 0.05$) violations of linear model assumptions were found.

Results

Demographics, cognitive measures and the mean GFC-R index values for the training and test sample are depicted in Table 1. The GFC-R index was not related to age in both samples.

GFC distribution

Figure 3 shows the spatial distribution of significant GFC values in the brain displayed in percentiles for the training (ADNI) and the test sample (ISD). We found a high spatial correspondence of significant GFC values between both samples with a correlation coefficient of $r = 0.84$, $p < 0.001$. The highest GFC values were observed predominantly within the frontal cortex, lateral parietal cortex, and areas of the medial brain surface. Those brain areas are known to be part of the DMN and the cognitive control network as reported previously (Cole et al. 2010).

Table 1 Demographics and neuropsychological characteristics of the study samples subjects split by Diagnosis and CR group

	Training sample (ADNI)			
	HC CR– (<i>n</i> = 13)	HC CR+ (<i>n</i> = 11)	MCI CR– (<i>n</i> = 24)	MCI CR+ (<i>n</i> = 19)
Age (years) ^a	75.12 ± 5.85	74.30 ± 7.56	74.90 ± 5.87	69.10 ± 6.16
Gender (female/male)	3/10	5/6	14/10	12/7
Education ^{b,c}	15.15 ± 1.41	18.64 ± 1.12	14.17 ± 1.58	18.58 ± 1.02
Global AV45 Uptake	0.99 ± 0.45	0.98 ± 0.04	1.4 ± 0.18	1.37 ± 0.15
MMSE ^{a,c}	29.12 ± 0.91	27.91 ± 1.45	26.71 ± 1.63	28.16 ± 1.34
RAVLT Learning ^b	45 ± 13.46	43.74 ± 7.81	31.71 ± 9.40	38.70 ± 8.91
	Test sample (ISD)			
	HC CR– (<i>n</i> = 17)	HC CR+ (<i>n</i> = 15)	MCI CR– (<i>n</i> = 13)	MCI CR+ (<i>n</i> = 10)
Age (years)	70.17 ± 3.94	72.52 ± 6.33	77.02 ± 3.63	73.87 ± 4.23
Gender ^d (female/male)	13/4	5/10	11/2	8/2
Education ^{b,c}	11.59 ± 1.33	16.6 ± 2.1	10.92 ± 1.98	17.1 ± 2.08
MMSE ^b	29.53 ± 0.87	29.33 ± 0.72	25.15 ± 1.52	27.9 ± 2.33
CERAD Word List Learning ^b	23 ± 2.6	24.07 ± 3.24	13.3 ± 2.84	18.9 ± 3.14

^a MCI CR+ < MCI CR–^b MCI CR+ > MCI CR–^c HC CR+ > HC CR–^d HC CR+ < HC CR–

The GFC-reserve index is decreased in MCI CR– as compared to MCI CR+

MCI CR– showed significantly lower GFC-R index values than the MCI CR+ subjects in the training sample ($F(7,35) = 17.82, p = 0.0001$; see Fig. 4a) and the test sample ($F(6,16) = 7.50, p = 0.015$). In an exploratory regression analysis in the training sample, we tested the association between the global AV45 uptake, WMH volume and the GFC-R index of the cognitive control network with age, gender, grey matter volume of the cognitive control network and the RAVLT learning score as covariates of no interest. The model showed no significant relationship between AV45 and the GFC-R index or between WMH volume and the GFC-R index. Similarly, in the test sample, WMH volume did not predict the GFC-R index, controlling for age, gender, CERAD word list learning and grey matter volume of the cognitive control network.

ROC analysis

Using a ROC analysis, we evaluated how accurate the GFC-reserve index discriminated between MCI CR+ and MCI CR– subjects (Fig. 4b). The AUC was 0.840 with the 95 % CI ranging between 0.72 and 0.95 within the training sample. Similarly, in the test sample, we found a AUC of 0.79 with the CI ranging from 0.60 to 0.99.

The GFC-reserve index is a predictor of CR proxies in the ISD test sample

Using linear regression, we tested whether the GFC-R index predicted CR proxies in the test sample, when controlling for age, gender, the word list learning score of the CERAD battery, WMH volume and grey matter volume of the cognitive control network. For years of education, the regression model was significant ($F(6,16) = 10.12, p = 0.0001$) with an adjusted R^2 of 0.71, showing that a higher GFC-R index significantly predicted higher years of education ($t(16) = 2.225, p = 0.041$). For the CRIq score, a higher GFC-R index predicted a higher CRIq score ($t(16) = 2.581, p = 0.020$, overall model fit: $F(6,16) = 3.498, p = 0.021$, adjusted R^2 0.41). The relationship between the GFC-R index and the CR proxies is illustrated in Fig. 5. When testing the Pearson-moment correlation between the GFC-R index and our CR proxies, the correlation was significant for both years of education ($r = 0.46, p = 0.026$) and the CRIq ($r = 0.6, p = 0.0024$).

The GFC-reserve index is specific to CR proxies

In linear regression analyses, we tested whether the GFC-R index is associated with better cognitive performance. We did not find the GFC-R index to predict RAVLT learning (ADNI), CERAD word list learning (ISD), or MMSE (ADNI & ISD) scores, controlling for age, gender, WMH volume and grey matter volume of the cognitive control network.

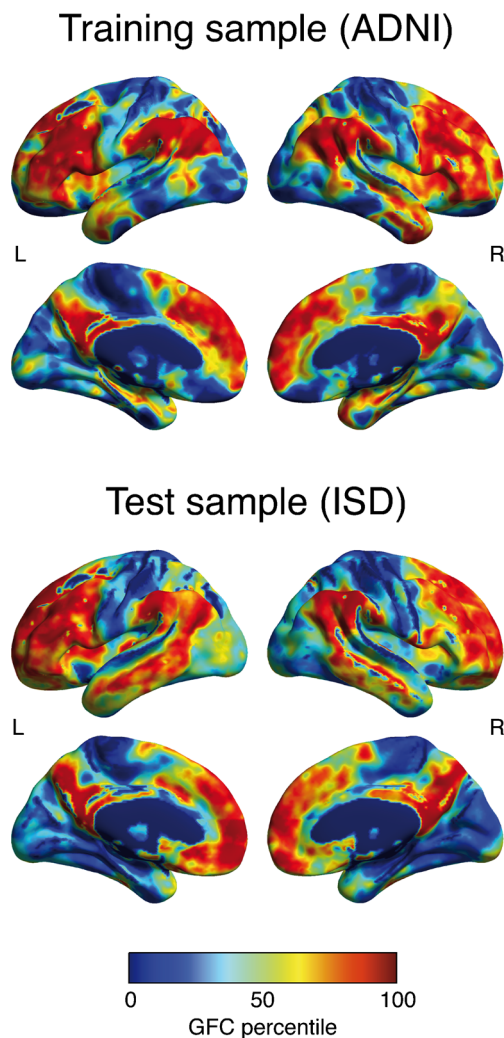


Fig. 3 Distribution of significant GFC values in the brain. T-values of voxel wise one-sample t-tests of the GFC among the pooled HC and MCI subjects (FWE corrected at the voxel level at $\alpha=0.001$) were converted to percentiles to facilitate visual group comparison between both samples

Control analyses in other brain networks

In order to test, whether our findings on the prediction of years of education by GFC-R index were specific for the cognitive control network, we repeated the regression analysis for GFC-R index derived from each of seven other major cortical networks (Yeo et al. 2011). For none of the other networks, the GFC-R index predicted years of education or the CRIq ($p > 0.05$, Table 2). This suggests that the relationship between GFC changes and education is specific for the cognitive control network.

Discussion

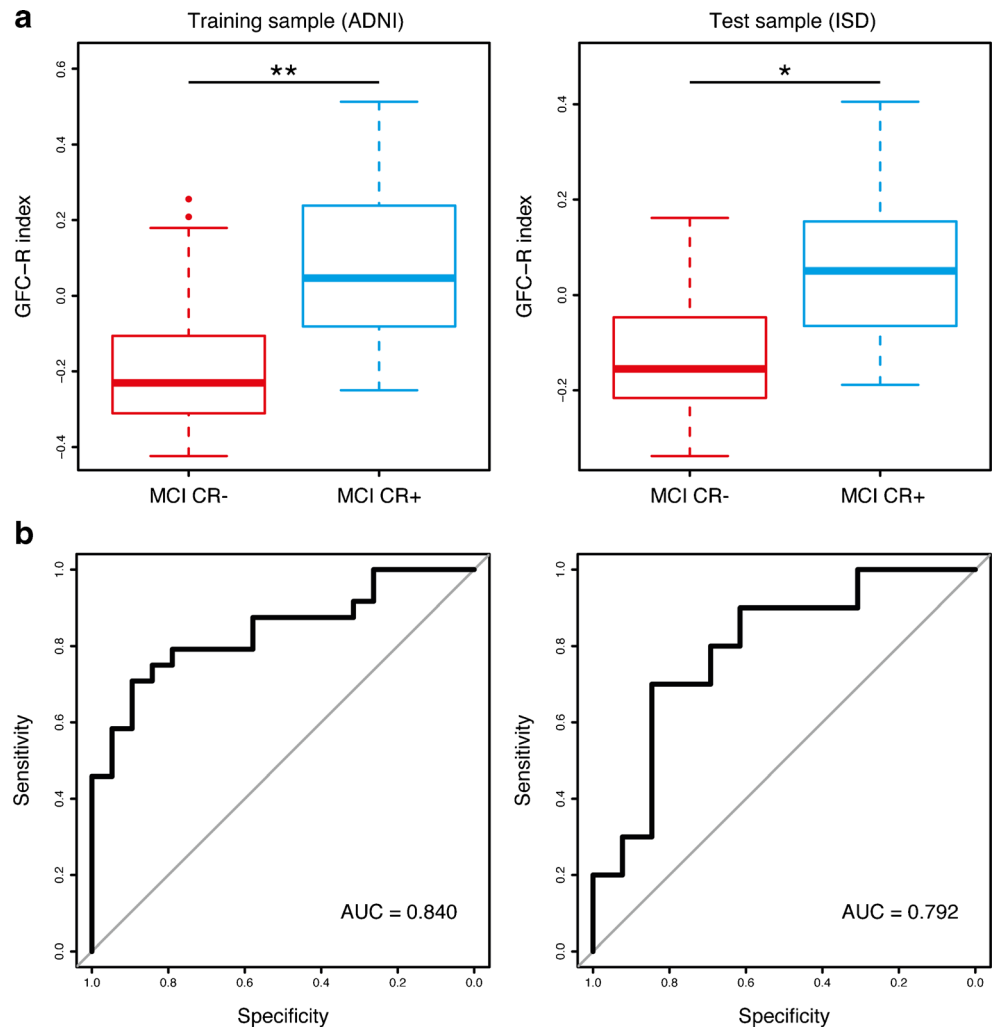
The first major finding of the current study was that MCI subjects with high CR (as measured by years of education)

had an increased frequency of high GFC values within the cognitive control network compared to MCI subjects with lower years of education. Secondly, a newly derived summary measure of abnormal GFC frequencies within the cognitive control network, the GFC-R index, showed a linear association with more years of education and a higher CRIq score, a composite measure of CR, in an independent cross-validation sample of MCI patients. The predictive value of GFC-R index was independent of demographic variables including age and gender, episodic memory performance, grey matter volume of the cognitive control network or WMH volume as a proxy of cerebral small vessel disease. These results suggest that the GFC-R index constitutes a biomarker candidate of CR-related functional brain changes in MCI.

For our first major finding, MCI CR+ showed a right-ward shift of the GFC histogram to that in HC CR+, i.e. MCI CR+ showed an increased frequency of relatively high GFC values. In contrast, there was a left-ward shift of the GFC histogram in the MCI CR- group, i.e. an increased frequency of lower GFC values. A previous study on GFC changes in MCI reported decreased GFC in the frontal, parietal, and temporal cortices in MCI (J. Wang et al. 2013). That latter study, however, did not assess the impact of years of education on GFC differences. Our results extend those previous results showing that the levels of CR are an important modifying factor, where MCI CR- subjects show a decrease in GFC but MCI CR+ subjects show an increase in GFC within the cognitive control network.

The increase in the frequency of high GFC values in MCI CR+ may reflect either pre-existing high levels of GFC before the development of MCI or, alternatively, a compensatory increase in GFC during the development of MCI, or thirdly, a dedifferentiation of functional connectivity that is related to pathological brain changes (Cabeza et al. 2002; Jones et al. 2011). Previous studies showed that higher IQ is associated with higher GFC within the left frontal core region of the cognitive control network in young subjects (Cole et al. 2012). Given that years of education and IQ are correlated (Matarazzo and Hermann 1984), it is possible that MCI CR+ subjects had already higher levels of GFC before disease onset, thus possessing higher brain reserve. However, the fact that MCI CR+ subjects showed abnormally increased frequency of high GFC values when compared to HC CR+, i.e. at similarly high levels of education, suggests a compensatory increase of GFC in MCI. Such an interpretation of compensatory increase of GFC in MCI is consistent with several previous studies showing increased resting-state functional connectivity in MCI and AD compared to HC (K. Wang et al. 2007), that is attributable to higher levels of education (Bozzali et al. 2015). On the other hand, the lacking relationship between the GFC-R index and cognitive performance partly challenge the notion that GFC increases are compensatory. A third possible explanation for an increase in GFC is a dedifferentiation of

Fig. 4 **a** Boxplots of the GFC-R index split by CR group for the training and the test sample. MCI CR- subjects show significantly lower GFC-CR values as MCI CR+ subjects in both samples. **b** shows the ROC curves with the specificity on the x- and the sensitivity on the y-axis. *AUC* Area under the curve, * = $p < 0.05$, ** = $p < 0.001$



functional connectivity due to pathological brain changes as suggested previously (Cabeza et al. 2002; Jones et al. 2011). However, we did not find GFC increases to be related to grey matter atrophy, WMH volume or amyloid deposition. Thus, our results indicate that the observed increase in GFC is unlikely to reflect pathology-driven dedifferentiation of functional connectivity. In summary, the MCI CR+ subjects

specifically show increased frequency of high GFC values within the cognitive control network, which could reflect compensatory changes in MCI, however this needs to be further investigated by future studies.

For our second major finding, we could show in a cross-validation approach that higher levels of the GFC-R index allow accurate point prediction of higher levels of education

Fig. 5 Scatterplot for the relationship between the GFC-R index and the CR proxies (years of education & CRtq) in the test sample

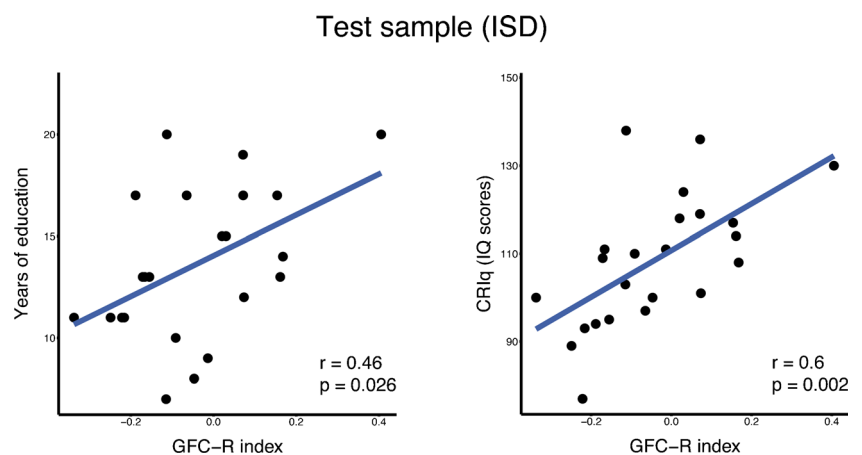


Table 2 Control analyses of the GFC-R index as a predictor of CR proxies in major brain networks

Functional network	Training sample (ADNI)		Test sample (ISD)			
	GFC-Diff		GFC-CR as a predictor of education in MCI CR+ and CR- pooled ¹		GFC-CR as a predictor of CRIq in MCI CR+ and CR- pooled ¹	
	CR+ < CR-	CR+ > CR-	T	p	T	p
Cognitive control	0.2–0.26	0.34–0.5	2.225	0.041	2.581	0.020
Default mode	0.2–0.27	0.37–0.52	0.631	0.537	1.324	0.204
Dorsal attention	0.22–0.28	0.41–0.51	0.998	0.333	0.934	0.364
Ventral attention	0.19–0.23	0.3–0.5	0.885	0.389	1.767	0.096
Frontoparietal	0.2–0.27	0.35–0.52	1.284	0.216	1.635	0.122
Limbic	0.25	0.36–0.46	0.644	0.529	0.577	0.572
Visual	0.22–0.28	0.43–0.53	0.255	0.801	1.526	0.147
Somatomotor	0.21–0.28	0.32–0.46	1.078	0.30	0.995	0.335

¹ Models controlled for age, gender, WMH volume, grey matter volume of the tested network, CERAD Word list learning score

and CRIq in MCI and could well separate high vs. low education groups in MCI as shown by the ROC analysis, with an AUC of 0.79. Note however that sensitivity and specificity is not of primary clinical significance in the context of CR, which is likely to be continuously distributed. More importantly, the GFC-R index showed a significant linear relationship with two different CR proxies in the validation sample. The point prediction is difficult but clinically important as previous studies showed that with each additional year of education, the onset of dementia is delayed by 0.21 years (Hall et al. 2007) and the risk of AD dementia is reduced (Sando et al. 2008; Stern et al. 1994). A critical test in the future will be whether the GFC-R index predicts slower cognitive decline in subjects with preclinical AD or MCI as has been reported for years of education as a proxy of CR (Soldan et al. 2015). The advantage of using fMRI based CR biomarkers such as GFC-R in such prediction models is that GFC-R could be used as a measure to track CR changes over time. CR may be reduced as the disease progresses since brain pathology may eventually use up the reserve (Members et al. 2010). In contrast, proxies of CR such as education or occupational attainment are time-invariant.

We found that only the GFC-R index derived from GFC values within the cognitive control network but not within any of the other major resting-state networks did significantly predict years of education or CRIq. For the ventral attention network, we found a trend level association between the GFC-R index and the CRIq, suggesting that the ventral attention network is to a certain extent associated with CR-related GFC increases. From a functional viewpoint, the ventral attention network is hypothesized to be involved in attentional control via coupling with other networks such as the dorsal attention or cognitive control network (Vossel et al. 2014). Similar to the cognitive control network, the ventral attention network

shows task-related hyperactivations in MCI and AD, as revealed by a recent meta-analysis of task-fMRI studies (Li et al. 2015). This suggests, that the ventral attention network is potentially involved in compensatory brain changes in MCI and AD. However, given that there was only a trend level association with one of the two CR proxies tested, we think that the role of the ventral attention network for the assessment of CR-related brain changes is questionable and requires further validation in future studies. Our results are broadly consistent with previous findings showing that higher GFC of brain regions in the cognitive control network but not the default mode network were predictive of higher IQ in healthy subjects (Cole et al. 2012). A possible explanation includes that the cognitive control network has a unique role in the brain, such that it is highly connected with the other networks and may orchestrate the activation of other networks during cognitive tasks (Cole et al. 2013, 2014b). Brain regions with increased connectedness in the brain have previously shown to be more resilient to targeted attacks as shown in graph theoretical analysis of resting-state fMRI (Achard et al. 2006). Higher GFC of the cognitive control network may enable to more flexibly activate different networks during cognitive processing (Cole et al. 2013), which in neurodegenerative disease may render a more flexible coping with local damage of specific neural networks such as the DMN (Greicius et al. 2004; Mevel et al. 2011), thus increasing CR. This will need to be tested in future combined resting-state and task-related fMRI studies.

We used years of education as our primary outcome measure, i.e. the gold standard, since educational attainment has been recommended as the best validated indicator of cognitive reserve (Stern 2012). Years of education has been tested as a CR proxy in numerous studies in AD (for review see (Stern 2012)) and is robustly associated with reduced risk of AD

dementia across studies (Meng and D’Arcy 2012; Valenzuela and Sachdev 2006). Alternative proxy measures of CR include assessments such as occupational attainment, premorbid IQ or leisure activities. Since we used international cross-validation samples, equivalent measures of such variables were not available in both samples in the current study. However, in the test sample, we found a significant positive association between the GFC-R index and the CRIq (Nucci et al. 2012) an alternative CR proxy that takes into account education, working and leisure activities, supporting criterion validity of the GFC-R index.

A promising alternative marker of CR has been recently proposed, consisting of the residual episodic memory variability after accounting for brain atrophy and demographic variables (Reed et al. 2010; Zahodne et al. 2013, 2015). Such a measure captures well CR as the discrepancy between the level of cognitive performance and brain pathology, but is non-informative about any structural or functional brain changes that may underlie CR. The current GFC-R index captures functional brain changes related to CR in MCI and would thus be complimentary to such memory-variance based marker or any of the standard proxy measures of CR.

For the interpretation of the current results several caveats need to be taken into account. It is important to note that the GFC-R index is not a biomarker candidate of CR per se, rather it is a biomarker of functional brain changes that are associated with CR in subjects with MCI. Ideally, the primary outcome parameter for the validation of the current biomarker constitute specific functional mechanisms that cause CR in MCI. Although several task fMRI studies have attempted to extract specific functional brain changes of CR in subjects with MCI and AD, no core mechanism, however, has yet emerged (for review see (Barulli and Stern 2013)). Thus, more work is needed to disentangle the functional brain processes that underlie CR, which could then provide a point of reference for the validation of functional biomarkers of CR in MCI. Still, years of education has been validated in numerous studies as a marker of CR and may thus constitute the best primary outcome as a reference measures for the validation of functional biomarkers of CR at this point.

It should be also taken into account that the reliability of GFC assessment is an important factor for the utility of GFC-R as a CR biomarker in MCI. Previous studies showed that GFC exhibits a fair to excellent test-retest reliability and its retest reliability ranks among the highest of resting-state fMRI functional connectivity measures (Liao et al. 2013; J. H. Wang et al. 2011). Multicenter variability of resting-state fMRI is an active field of research and needs still to be established for the various connectivity indices including that of GFC. However, the current cross-validation of the GFC-R between different samples suggest robustness of the current findings (Feis et al. 2015). Moreover, both samples were scanned on different

scanners with different scanner protocols, but still results were highly comparable. This favors the use of the GFC-R index as a fMRI-based marker of CR in MCI that can be validly assessed across sites and scanners. Summary indices that average across a large number of voxels such as the GFC-R index may be more robust to multicenter variability than measures focusing on small ROIs (Ewers et al. 2006). Still, the test-retest and multicenter variability of the GFC-R index needs to be established in future studies, however, our analysis renders the GFC-R index a promising candidate marker of CR that can be robustly assessed across different scanner protocols.

A strength of the current approach is the fully automated way to extract GFC frequency changes in MCI based on resting-state fMRI. Thus, functional MRI data can be assessed without reliance on a task and data processing can be done without manual intervention, which provides a high attractiveness to be used in clinical praxis. Possible clinical applications of the GFC-R index as diagnostic biomarker candidate include the use as an outcome measure in clinical trials such as cognitive training, physical training that target compensatory brain mechanisms to prevent conversion from MCI to AD dementia (Suo et al. 2016). Secondly, the GFC-R index could be used to track changes in CR during the progression of the disease. Future longitudinal studies may address these next steps.

Compliance with ethical standards The study at the ISD was approved by the ethics committee of the Ludwig Maximilian University of Munich. For the ADNI-sample ethical approval was obtained by the ADNI investigators. All procedures performed were in accordance with the ethical standards of the institutional and/or national research committee and with the 1964 Helsinki declaration and its later amendments or comparable ethical standards. All study participants provided written, informed consent to the study.

Funding The research was funded by grants of the LMUexcellent Initiative and the European Commission (ERC, PCIG12-GA-2012-334259), Alzheimer’s Forschung Initiative (AFI, DE-15035). Data collection and sharing for this project was funded by the Alzheimer’s Disease Neuroimaging Initiative (ADNI) (National Institutes of Health Grant U01 AG024904) and DOD ADNI (Department of Defense award number W81XWH-12-2-0012). ADNI is funded by the National Institute on Aging, the National Institute of Biomedical Imaging and Bioengineering, and through generous contributions from the following: AbbVie, Alzheimer’s Association; Alzheimer’s Drug Discovery Foundation; Araclon Biotech; BioClinica, Inc.; Biogen; Bristol-Myers Squibb Company; CereSpir, Inc.; Eisai Inc.; Elan Pharmaceuticals, Inc.; Eli Lilly and Company; EuroImmun; F. Hoffmann-La Roche Ltd and its affiliated company Genentech, Inc.; Fujirebio; GE Healthcare; IXICO Ltd.; Janssen Alzheimer Immunotherapy Research & Development, LLC.; Johnson & Johnson Pharmaceutical Research & Development LLC.; Lumosity; Lundbeck; Merck & Co., Inc.; Meso Scale Diagnostics, LLC.; NeuroRx Research; Neurotrack Technologies; Novartis Pharmaceuticals Corporation; Pfizer Inc.; Piramal Imaging; Servier; Takeda Pharmaceutical Company; and Transition Therapeutics. The Canadian Institutes of Health Research is providing funds to support ADNI clinical sites in Canada. Private sector contributions are facilitated by the Foundation for the National Institutes of Health (www.fnih.org).

The grantee organization is the Northern California Institute for Research and Education, and the study is coordinated by the Alzheimer's Disease Cooperative Study at the University of California, San Diego. ADNI data are disseminated by the Laboratory for Neuro Imaging at the University of Southern California.

Conflict of interest The authors declare that they have no conflict of interest

References

- Achard, S., Salvador, R., Whitcher, B., Suckling, J., & Bullmore, E. (2006). A resilient, low-frequency, small-world human brain functional network with highly connected association cortical hubs. *Journal of Neuroscience*, 26(1), 63–72. doi:10.1523/JNEUROSCI.3874-05.2006.
- Arenaza-Urquijo, E. M., Landeau, B., La Joie, R., Mevel, K., Mezenge, F., Perrotin, A., & Chetelat, G. (2013). Relationships between years of education and gray matter volume, metabolism and functional connectivity in healthy elders. *NeuroImage*, 83, 450–457. doi:10.1016/j.neuroimage.2013.06.053.
- Ashburner, J. (2007). A fast diffeomorphic image registration algorithm. *NeuroImage*, 38(1), 95–113. doi:10.1016/j.neuroimage.2007.07.007.
- Ashburner, J., & Friston, K. J. (2005). Unified segmentation. *NeuroImage*, 26(3), 839–851. doi:10.1016/j.neuroimage.2005.02.018.
- Barulli, D., & Stern, Y. (2013). Efficiency, capacity, compensation, maintenance, plasticity: emerging concepts in cognitive reserve. *Trends in Cognitive Sciences*, 17(10), 502–509. doi:10.1016/j.tics.2013.08.012.
- Bastin, C., Yakushev, I., Bahri, M. A., Fellgiebel, A., Eustache, F., Landeau, B., & Salmon, E. (2012). Cognitive reserve impacts on inter-individual variability in resting-state cerebral metabolism in normal aging. *NeuroImage*, 63(2), 713–722. doi:10.1016/j.neuroimage.2012.06.074.
- Boots, E. A., Schultz, S. A., Almeida, R. P., Oh, J. M., Kosciak, R. L., Dowling, M. N., & Okonkwo, O. C. (2015). Occupational complexity and cognitive reserve in a middle-aged cohort at risk for Alzheimer's disease. *Archives of Clinical Neuropsychology*. doi:10.1093/arclin/acv041.
- Bosch, B., Bartres-Faz, D., Rami, L., Arenaza-Urquijo, E. M., Fernandez-Espejo, D., Junque, C., & Molinuevo, J. L. (2010). Cognitive reserve modulates task-induced activations and deactivations in healthy elders, amnesic mild cognitive impairment and mild Alzheimer's disease. *Cortex*, 46(4), 451–461. doi:10.1016/j.cortex.2009.05.006.
- Bozzali, M., Dowling, C., Serra, L., Spano, B., Torso, M., Marra, C., & Cercignani, M. (2015). The impact of cognitive reserve on brain functional connectivity in Alzheimer's disease. *Journal of Alzheimer's Disease*, 44(1), 243–250. doi:10.3233/JAD-141824.
- Brickman, A. M., Siedlecki, K. L., Muraskin, J., Manly, J. J., Luchsinger, J. A., Yeung, L. K., & Stern, Y. (2011). White matter hyperintensities and cognition: testing the reserve hypothesis. *Neurobiology of Aging*, 32(9), 1588–1598. doi:10.1016/j.neurobiolaging.2009.10.013.
- Buschert, V. C., Friese, U., Teipel, S. J., Schneider, P., Merensky, W., Rujescu, D., & Buerger, K. (2011). Effects of a newly developed cognitive intervention in amnesic mild cognitive impairment and mild Alzheimer's disease: a pilot study. *Journal of Alzheimer's Disease*, 25(4), 679–694. doi:10.3233/JAD-2011-100999.
- Cabeza, R., Anderson, N. D., Locantore, J. K., & McIntosh, A. R. (2002). Aging gracefully: compensatory brain activity in high-performing older adults. *NeuroImage*, 17(3), 1394–1402. Retrieved from <http://www.ncbi.nlm.nih.gov/pubmed/12414279> http://ac.els-cdn.com/S1053811902912802/1-s2.0-S1053811902912802-main.pdf?_tid=47765b2a-94f7-11e3-b99e-00000aacb35d&acdnt=1392327732_9b8b93ea71e8f450a6a07dc8e9dace8c.
- Cole, M. W., & Schneider, W. (2007). The cognitive control network: integrated cortical regions with dissociable functions. *NeuroImage*, 37(1), 343–360. doi:10.1016/j.neuroimage.2007.03.071.
- Cole, M. W., Pathak, S., & Schneider, W. (2010). Identifying the brain's most globally connected regions. *NeuroImage*, 49(4), 3132–3148. doi:10.1016/j.neuroimage.2009.11.001.
- Cole, M. W., Yarkoni, T., Repovs, G., Anticevic, A., & Braver, T. S. (2012). Global connectivity of prefrontal cortex predicts cognitive control and intelligence. *Journal of Neuroscience*, 32(26), 8988–8999. doi:10.1523/JNEUROSCI.0536-12.2012.
- Cole, M. W., Reynolds, J. R., Power, J. D., Repovs, G., Anticevic, A., & Braver, T. S. (2013). Multi-task connectivity reveals flexible hubs for adaptive task control. *Nature Neuroscience*, 16(9), 1348–1355. doi:10.1038/nn.3470.
- Cole, M. W., Bassett, D. S., Power, J. D., Braver, T. S., & Petersen, S. E. (2014a). Intrinsic and task-evoked network architectures of the human brain. *Neuron*, 83(1), 238–251. doi:10.1016/j.neuron.2014.05.014.
- Cole, M. W., Repovs, G., & Anticevic, A. (2014b). The frontoparietal control system: a central role in mental health. *The Neuroscientist*, 20(6), 652–664. doi:10.1177/1073858414525995.
- Elman, J. A., Oh, H., Madison, C. M., Baker, S. L., Vogel, J. W., Marks, S. M., & Jagust, W. J. (2014). Neural compensation in older people with brain amyloid-beta deposition. *Nature Neuroscience*, 17(10), 1316–1318. doi:10.1038/nn.3806.
- Ewers, M., Teipel, S. J., Dietrich, O., Schonberg, S. O., Jessen, F., Heun, R., & Hampel, H. (2006). Multicenter assessment of reliability of cranial MRI. *Neurobiology of Aging*, 27(8), 1051–1059. doi:10.1016/j.neurobiolaging.2005.05.032.
- Ewers, M., Brendel, M., Rizk-Jackson, A., Rominger, A., Bartenstein, P., Schuff, N., & Alzheimer's Disease Neuroimaging I. (2014). Reduced FDG-PET brain metabolism and executive function predict clinical progression in elderly healthy subjects. *NeuroImage Clinical*, 4, 45–52. doi:10.1016/j.nicl.2013.10.018.
- Feis, R. A., Smith, S. M., Filippini, N., Douaud, G., Dopper, E. G., Heise, V., & Mackay, C. E. (2015). ICA-based artifact removal diminishes scan site differences in multi-center resting-state fMRI. *Frontiers in Neuroscience*, 9, 395. doi:10.3389/fnins.2015.00395.
- Greicius, M. D., Srivastava, G., Reiss, A. L., & Menon, V. (2004). Default-mode network activity distinguishes Alzheimer's disease from healthy aging: evidence from functional MRI. *Proceedings of the National Academy of Sciences of the United States of America*, 101(13), 4637–4642. doi:10.1073/pnas.0308627101.
- Hall, C. B., Derby, C., LeValley, A., Katz, M. J., Verghese, J., & Lipton, R. B. (2007). Education delays accelerated decline on a memory test in persons who develop dementia. *Neurology*, 69(17), 1657–1664. doi:10.1212/01.wnl.0000278163.82636.30.
- Jones, D. T., Machulda, M. M., Vemuri, P., McDade, E. M., Zeng, G., Senjem, M. L., & Jack, C. R., Jr. (2011). Age-related changes in the default mode network are more advanced in Alzheimer disease. *Neurology*, 77(16), 1524–1531. doi:10.1212/WNL.0b013e318233b33d.
- Landau, S. M., Breault, C., Joshi, A. D., Pontecorvo, M., Mathis, C. A., Jagust, W. J., & Alzheimer's Disease Neuroimaging I. (2013). Amyloid-beta imaging with Pittsburgh compound B and florbetapir: comparing radiotracers and quantification methods. *Journal of Nuclear Medicine*, 54(1), 70–77. doi:10.2967/jnumed.112.109009.
- Li, H. J., Hou, X. H., Liu, H. H., Yue, C. L., He, Y., & Zuo, X. N. (2015). Toward systems neuroscience in mild cognitive impairment and Alzheimer's disease: a meta-analysis of 75 fMRI studies. *Human Brain Mapping*, 36(3), 1217–1232. doi:10.1002/hbm.22689.
- Liao, X. H., Xia, M. R., Xu, T., Dai, Z. J., Cao, X. Y., Niu, H. J., & He, Y. (2013). Functional brain hubs and their test-retest reliability: a multiband resting-state functional MRI study. *NeuroImage*, 83, 969–982. doi:10.1016/j.neuroimage.2013.07.058.

- Luck, T., Riedel-Heller, S., & Wiese, B. (2009). CERAD-NP-Testbatterie: Alters-, geschlechts- und bildungsspezifischen Normen ausgewählter Subtests. *Zeitschrift für Gerontologie und Geriatrie*, *42*, 372–384.
- Matarazzo, J. D., & Hermann, D. O. (1984). The relationship of education and IQ in the WAIS-R standardization sample. *Journal of Consulting and Clinical Psychology*, *52*(4), 631–634.
- Members, E. C. C., Brayne, C., Ince, P. G., Keage, H. A., McKeith, I. G., Matthews, F. E., & Sulkava, R. (2010). Education, the brain and dementia: neuroprotection or compensation? *Brain*, *133*(Pt 8), 2210–2216. doi:10.1093/brain/awq185.
- Meng, X., & D'Arcy, C. (2012). Education and dementia in the context of the cognitive reserve hypothesis: a systematic review with meta-analyses and qualitative analyses. *PLoS ONE*, *7*(6), e38268. doi:10.1371/journal.pone.0038268.
- Mevel, K., Chetelat, G., Eustache, F., & Desgranges, B. (2011). The default mode network in healthy aging and Alzheimer's disease. *International Journal of Alzheimer's Disease*, *2011*, 535816. doi:10.4061/2011/535816.
- Nucci, M., Mapelli, D., & Mondini, S. (2012). Cognitive reserve index questionnaire (CRIq): a new instrument for measuring cognitive reserve. *Aging Clinical and Experimental Research*, *24*(3), 218–226. doi:10.3275/7800.
- Oh, H., Steffener, J., Razlighi, Q. R., Habeck, C., Liu, D., Gazes, Y., & Stern, Y. (2015). Abeta-related hyperactivation in frontoparietal control regions in cognitively normal elderly. *Neurobiology of Aging*, *36*(12), 3247–3254. doi:10.1016/j.neurobiolaging.2015.08.016.
- Otsu, N. (1979). A thresholding selection method from gray-level histogram. *IEEE Transactions on Systems, Man, and Cybernetics*, *9*.
- Petersen, R. C. (2004). Mild cognitive impairment as a diagnostic entity. *Journal of Internal Medicine*, *256*(3), 183–194. doi:10.1111/j.1365-2796.2004.01388.x.
- R Development Core Team. (2013). *R: A language and environment for statistical computing*. Vienna: R Foundation for Statistical Computing.
- Reed, B. R., Mungas, D., Farias, S. T., Harvey, D., Beckett, L., Widaman, K., & DeCarli, C. (2010). Measuring cognitive reserve based on the decomposition of episodic memory variance. *Brain*, *133*(Pt 8), 2196–2209. doi:10.1093/brain/awq154.
- Reijnders, J., van Heugten, C., & van Boxtel, M. (2013). Cognitive interventions in healthy older adults and people with mild cognitive impairment: a systematic review. *Ageing Research Reviews*, *12*(1), 263–275. doi:10.1016/j.arr.2012.07.003.
- Rentz, D. M., Locascio, J. J., Becker, J. A., Moran, E. K., Eng, E., Buckner, R. L., & Johnson, K. A. (2010). Cognition, reserve, and amyloid deposition in normal aging. *Annals of Neurology*, *67*(3), 353–364. doi:10.1002/ana.21904.
- Sando, S. B., Melquist, S., Cannon, A., Hutton, M., Sletvold, O., Saltvedt, I., & Aasly, J. (2008). Risk-reducing effect of education in Alzheimer's disease. *International Journal of Geriatric Psychiatry*, *23*(11), 1156–1162. doi:10.1002/gps.2043.
- Scarmeas, N., Zarahn, E., Anderson, K. E., Habeck, C. G., Hilton, J., Flynn, J., & Stern, Y. (2003). Association of life activities with cerebral blood flow in Alzheimer disease: implications for the cognitive reserve hypothesis. *Arch Neurol*, *60*(3), 359–365. Retrieved from <http://www.ncbi.nlm.nih.gov/pubmed/12633147>.
- Schoenberg, M. R., Dawson, K. A., Duff, K., Patton, D., Scott, J. G., & Adams, R. L. (2006). Test performance and classification statistics for the Rey auditory verbal learning test in selected clinical samples. *Archives of Clinical Neuropsychology*, *21*(7), 693–703. doi:10.1016/j.acn.2006.06.010.
- Schultz, S. A., Larson, J., Oh, J., Kosciak, R., Dowling, M. N., Gallagher, C. L., & Okonkwo, O. C. (2015). Participation in cognitively-stimulating activities is associated with brain structure and cognitive function in preclinical Alzheimer's disease. *Brain Imaging and Behavior*, *9*(4), 729–736. doi:10.1007/s11682-014-9329-5.
- Soldan, A., Pettigrew, C., Lu, Y., Wang, M. C., Selnes, O., Albert, M., & Team, B. R. (2015). Relationship of medial temporal lobe atrophy, APOE genotype, and cognitive reserve in preclinical Alzheimer's disease. *Human Brain Mapping*, *36*(7), 2826–2841. doi:10.1002/hbm.22810.
- Solé-Padullés, C., Bartrés-Faz, D., Junqué, C., Vendrell, P., Rami, L., Clemente, I. C., & Molinuevo, J. L. (2009). Brain structure and function related to cognitive reserve variables in normal aging, mild cognitive impairment and Alzheimer's disease. *Neurobiology of Aging*, *30*(7), 1114–1124. Retrieved from <http://www.sciencedirect.com/science/article/pii/S0197458007004083>.
- Stern, Y. (2002). What is cognitive reserve? Theory and research application of the reserve concept. *J Int Neuropsychol Soc*, *8*(3), 448–460. Retrieved from <http://www.ncbi.nlm.nih.gov/pubmed/11939702>.
- Stern, Y. (2009). Cognitive reserve. *Neuropsychologia*, *47*(10), 2015–2028. doi:10.1016/j.neuropsychologia.2009.03.004.
- Stern, Y. (2012). Cognitive reserve in ageing and Alzheimer's disease. *Lancet Neurology*, *11*(11), 1006–1012. doi:10.1016/S1474-4422(12)70191-6.
- Stern, Y., Alexander, G. E., Prohovnik, I., & Mayeux, R. (1992). Inverse relationship between education and parietotemporal perfusion deficit in Alzheimer's disease. *Annals of Neurology*, *32*(3), 371–375. doi:10.1002/ana.410320311.
- Stern, Y., Gurland, B., Tatemichi, T. K., Tang, M. X., Wilder, D., & Mayeux, R. (1994). Influence of education and occupation on the incidence of Alzheimer's disease. *Jama*, *271*(13), 1004–1010. Retrieved from http://www.ncbi.nlm.nih.gov/entrez/query.fcgi?cmd=Retrieve&db=PubMed&dopt=Citation&list_uids=8139057.
- Stern, Y., Alexander, G. E., Prohovnik, I., Stricks, L., Link, B., Lennon, M. C., & Mayeux, R. (1995). Relationship between lifetime occupation and parietal flow: implications for a reserve against Alzheimer's disease pathology. *Neurology*, *45*(1), 55–60. Retrieved from <http://www.ncbi.nlm.nih.gov/pubmed/7824135>.
- Stern, Y., Habeck, C., Moeller, J., Scarmeas, N., Anderson, K. E., Hilton, H. J., & van Heertum, R. (2005). Brain networks associated with cognitive reserve in healthy young and old adults. *Cerebral Cortex*, *15*(4), 394–402. doi:10.1093/cercor/bhh142.
- Stern, Y., Zarahn, E., Habeck, C., Holtzer, R., Rakitin, B. C., Kumar, A., & Brown, T. (2008). A common neural network for cognitive reserve in verbal and object working memory in young but not old. *Cerebral Cortex*, *18*(4), 959–967. doi:10.1093/cercor/bhm134.
- Suo, C., Singh, M. F., Gates, N., Wen, W., Sachdev, P., Brodaty, H., & Valenzuela, M. J. (2016). Therapeutically relevant structural and functional mechanisms triggered by physical and cognitive exercise. *Molecular Psychiatry*. doi:10.1038/mp.2016.19.
- Valenzuela, M. J., & Sachdev, P. (2006). Brain reserve and dementia: a systematic review. *Psychological Medicine*, *36*(4), 441–454. doi:10.1017/S0033291705006264.
- Vemuri, P., Weigand, S. D., Przybelski, S. A., Knopman, D. S., Smith, G. E., Trojanowski, J. Q., & Alzheimer's Disease Neuroimaging I. (2011). Cognitive reserve and Alzheimer's disease biomarkers are independent determinants of cognition. *Brain*, *134*(Pt 5), 1479–1492. doi:10.1093/brain/awr049.
- Vemuri, P., Lesnick, T. G., Przybelski, S. A., Knopman, D. S., Preboske, G. M., Kantarci, K., & Jack, C. R., Jr. (2015). Vascular and amyloid pathologies are independent predictors of cognitive decline in normal elderly. *Brain*, *138*(Pt 3), 761–771. doi:10.1093/brain/awu393.
- Vossel, S., Geng, J. J., & Fink, G. R. (2014). Dorsal and ventral attention systems: distinct neural circuits but collaborative roles. *The Neuroscientist*, *20*(2), 150–159. doi:10.1177/1073858413494269.
- Wang, K., Liang, M., Wang, L., Tian, L., Zhang, X., Li, K., & Jiang, T. (2007). Altered functional connectivity in early Alzheimer's disease: a resting-state fMRI study. *Human Brain Mapping*, *28*(10), 967–978. doi:10.1002/hbm.20324.

- Wang, J. H., Zuo, X. N., Gohel, S., Milham, M. P., Biswal, B. B., & He, Y. (2011). Graph theoretical analysis of functional brain networks: test-retest evaluation on short- and long-term resting-state functional MRI data. *PLoS ONE*, *6*(7), e21976. doi:[10.1371/journal.pone.0021976](https://doi.org/10.1371/journal.pone.0021976).
- Wang, J., Zuo, X., Dai, Z., Xia, M., Zhao, Z., Zhao, X., & He, Y. (2013). Disrupted functional brain connectome in individuals at risk for Alzheimer's disease. *Biological Psychiatry*, *73*(5), 472–481. doi:[10.1016/j.biopsych.2012.03.026](https://doi.org/10.1016/j.biopsych.2012.03.026).
- Wells, R. E., Yeh, G. Y., Kerr, C. E., Wolkin, J., Davis, R. B., Tan, Y., & Kong, J. (2013). Meditation's impact on default mode network and hippocampus in mild cognitive impairment: a pilot study. *Neuroscience Letters*, *556*, 15–19. doi:[10.1016/j.neulet.2013.10.001](https://doi.org/10.1016/j.neulet.2013.10.001).
- Yarkoni, T., Poldrack, R. A., Nichols, T. E., Van Essen, D. C., & Wager, T. D. (2011). Large-scale automated synthesis of human functional neuroimaging data. *Nature Methods*, *8*(8), 665–670. doi:[10.1038/nmeth.1635](https://doi.org/10.1038/nmeth.1635).
- Yeo, B. T., Krienen, F. M., Sepulcre, J., Sabuncu, M. R., Lashkari, D., Hollinshead, M., & Buckner, R. L. (2011). The organization of the human cerebral cortex estimated by intrinsic functional connectivity. *Journal of Neurophysiology*, *106*(3), 1125–1165. doi:[10.1152/jn.00338.2011](https://doi.org/10.1152/jn.00338.2011).
- Zahodne, L. B., Manly, J. J., Brickman, A. M., Siedlecki, K. L., Decarli, C., & Stern, Y. (2013). Quantifying cognitive reserve in older adults by decomposing episodic memory variance: replication and extension. *Journal of International Neuropsychological Society*, *19*(8), 854–862. doi:[10.1017/S1355617713000738](https://doi.org/10.1017/S1355617713000738).
- Zahodne, L. B., Manly, J. J., Brickman, A. M., Narkhede, A., Griffith, E. Y., Guzman, V. A., & Stern, Y. (2015). Is residual memory variance a valid method for quantifying cognitive reserve? A longitudinal application. *Neuropsychologia*, *77*, 260–266. doi:[10.1016/j.neuropsychologia.2015.09.009](https://doi.org/10.1016/j.neuropsychologia.2015.09.009).